Available online at www.sciencedirect.com

ScienceDirect

Procedia Computer Science 42 (2014) 17 – 24

Procedia Computer Science

International Conference on Robot PRIDE 2013-2014 - Medical and Rehabilitation Robotics and Instrumentation, ConfPRIDE 2013-2014

Advanced Design of Columnar-conical Feeler-type Optical Three-axis Tactile Sensor

Masahiro Ohka[a]*, Akihiro Tsunogai[a], Takashi Kayaba[a], Sukarnur Che Abdullah[b], Hanafiah Yussof[b]

[a]*Nagoya University, Graduate School of Information Science, Furo-cho Chikusa-ku Nagoya 464-8601, Japan*
[b]*Center for Humanoid Robots and Bio-Sensing (HuRoBs), Faculty of Mechanical Engineering, Universiti Teknologi MARA, Malaysia*

Abstract

Although the three-axis tactile sensor is capable of delicate measurement, it is weak for heavy contact force. In order to enhance resistance to a high degree of applied force, we attached a rubber skin onto the sensor surface to protect the sensing element. FEM analyses found that sensitivity is not significantly reduced and that the skin induces subsidiary effects such as the disappearance of insensible areas and the enhancement of stability of the columnar feeler. If the skin is substantially softer than the columnar-conical feeler, the sensor can measure three-axis force without reduction of sensitivity. Based on these simulated results, we produced a columnar-conical feeler-type three-axis tactile sensor with rubber skin. The experimental results show, as demonstrated by FEM analyses, that the sensor possesses three-axis sensing capability and that the insensible area vanishes.

Peer-review under responsibility of the Center for Humanoid Robots and Bio-Sensing (HuRoBs)

Keywords: Robotics; Tactile sensor; Three-axis; Skin; Feeler-type; FEM

1. Introduction

Since three-axis tactile sensors are capable of simultaneously measuring normal and tangential forces, they attract many researchers in robotics[1]. Previous studies of the three-axis tactile sensor have presented several designs of

* Corresponding author. Tel.: +81-52-789-4861; fax: +81-52-781-4800.
*E-mail address:*ohka@is.nagoya-u.ac.jp

Peer-review under responsibility of the Center for Humanoid Robots and Bio-Sensing (HuRoBs)
doi:10.1016/j.procs.2014.11.028

multi-axis force cells based on such physical phenomena as magnetic effects[2], variations in electrical capacity[3,4], piezoelectric polyvinylidene difluoride (PVDF) film (piezoelectric effect)[5], and photointerrupters (variations in light)[6]. Recently, since the remarkable development of microelectromechanical systems (MEMS), several interesting projects have progressed the development of three-axis tactile sensors[7-9] that are expected to be used as artificial skin. The sensors based on MEMS have the potential to produce large-scale arrays composed of miniaturized sensing elements. Although the development of three-axis tactile sensors continues to advance, as mentioned above, almost all tactile sensors are developed as prototypes for analysis. Since they do not have sufficient cell array size or are not applied to actual robotic hands, they remain in the developmental stage. On the other hand, the image data processing-based tactile sensor (gel sensor), based on a similar principle to our sensor, can now detect three-axis force distribution[10]. However, this sensor requires appropriate direct calibration to obtain actual contact information because of the interference between cells.

To date, we have developed several types of optical three-axis tactile sensors, such as the columnar-conical feeler sensor[11,12] and the feeler movement sensor[13,14]. Although the former type is capable of delicate measurement, it is weak for heavy contact force. On the other hand, the latter sensor can endure relatively high pressure, but its three-axis force sensing precision is not as good as the columnar-conical feeler sensor. In order to enhance resistance to a high degree of applied force in the columnar-conical feeler type, we intend to attach a rubber skin onto the sensor surface to protect the sensing element from a high degree of applied force.

The ordinal theory[15] concluded that, since skin blurs stress distribution, the design of tactile sensors should take into account the trade-off between this blur effect and protection of the sensor elements. Since this theory was deduced using a simple sheet-type skin, we examined whether the theory can be applied to a more complex structure such as the present tactile sensor. Furthermore, we evaluated whether the skin induces subsidiary effects, such as the disappearance of insensible areas and enhancement of columnar feeler stability.

In this paper, we examine the principle of the abovementioned skin function using numerical simulations of the finite element method (FEM). According to the simulations, if the rubber skin possesses appropriate softness compared to the columnar-conical feelers acting as sensing elements, the sensor can measure three-axis force without a considerable reduction in sensitivity, even with thick skin. Based on the simulated results, we produced the columnar-conical feeler-type three-axis tactile sensor with rubber skin. Finally, we performed a series of experiments to show that the new sensor possesses three-axis sensing capability, as demonstrated by numerical simulation, and that the insensible area vanishes.

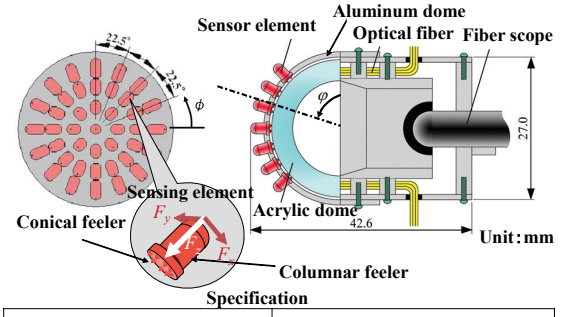

Specification

Number of elements	**41**
Detectable max. force / element	F_x, F_y: 0.15 N, F_z: 2 N
Acceptable max. force / element	F_x, F_y: 2 N, F_z: 3 N
Resolution	F_x, F_y: 1×10^{-5} N, F_z: 3.6×10^{-5} N

Fig. 1. Columnar-and-conical feeler-type three-axis tactile sensor[11,12]

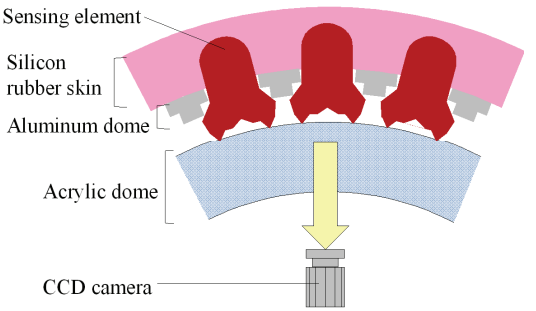

Fig. 2. Schematic design of tactile sensor

2. Design of Columnar-conical Feeler-type Tactile Sensor

2.1. Basic Sensing Principle

This type of sensor is comprised of a rubber sheet and a transparent acrylic plate illuminated along its edge by a light source[16]. The light, which is directed into the plate, remains within it due to the total internal reflection that is

generated. A rubber sheet featuring an array of conical feelers is placed on the plate to maintain array surface contact with the plate. If an object contacts the back of the rubber sheet, resulting in contact pressure, the feelers collapse and, at the points where they collapse, light is diffusely reflected out of the plate's reverse surface. The distribution of the contact pressure is calculated from the bright areas viewed from the reverse surface of the plate.

We designed complex structures comprised of two types of feeler arrays attached to opposite sides of the rubber sheet[17]. One is a sparse array of columnar feelers that makes contact with the object for recognition; the other is a dense array of conical feelers that maintains contact with the waveguide plate. Since each columnar feeler is arranged on several conical feelers so that it presses against the conical feelers under an applied force, three components of the force vector are identified by distribution of the conical feelers' contact areas.

In the columnar-conical feeler-type tactile sensor, normal and tangential forces are measured from an integrated grayscale value of the image data G and the centroid movement of the bright area, which is expressed by the u_x and u_y in local coordinates. We assume that three components of applied force, F_x, F_y, and F_z, are proportional to u_x, u_y, and G. Furthermore, we arrange the sensing elements on a hemispherical surface to apply our sensor onto a robotic fingertip (Fig. 1). This design extracts the interference between the sensing elements because each element in the array is independent.

2.2. Problem of Conventional Three-axis Tactile Sensor and Its Advanced Design

In previous studies[11,12], our conventional columnar-conical feeler-type optical three-axis tactile sensor had high sensitivity and resolution because it can measure 2 N and 0.15 N for normal and tangential directions, respectively, and it can distinguish 0.036 mN and 0.010 mN for variations in normal and tangential force, respectively. Additionally, since each of its sensing elements is isolated, 41 sensing elements can be calibrated with actual loading tests. As mentioned earlier, it is precise enough to measure applied force on a robotic finger.

However, this sensor is not always used for a high degree of applied force. If applied force for each sensing element exceeds approximately 2 N, all the conical feelers collapse to cause sensitivity saturation. Since about seven to eight elements are touching in most of our experiments performed thus far, each finger installed in this sensor can measure applied force up to 14-16 N. Although this force level is not always low for practical use, it is not enough for grasping heavy objects.

Additionally, since there is no sensing site between any two columnar feelers, this sensor cannot sense an object small enough to fit between two feelers. When a robotic finger equipped with this sensor grasps daily use objects that are smaller than the distance between two columnar feelers, it does not obtain tactile information. Furthermore, if a robot finger equipped with this sensor does clay work, the tips of the sensing element will become stuck in the clay. Although the human fingertip has a fingerprint, the protrusion of this sensor's sensing element is too large compared to the ridges of a fingerprint. In addition, the columnar feeler can occasionally be cut by the edge of an aluminum hole if a large tangential force is applied.

In order to overcome the abovementioned problems, we attached a rubber skin onto the top of the tactile sensor, as shown in Fig. 2. Although the rubber skin makes stimulation ambiguous, we assume that if we adopt appropriate skin softness as compared to the sensing element, the sensitivity of this sensor will not be problematically reduced. Furthermore, we assume that, even if we apply force between two sensing elements, the deformation flow of the soft rubber will push the neighboring sensing elements.

3. Computer Simulation Using FEM

3.1. FE Model for Tactile Sensor

In order to confirm the aforementioned scheme of the new sensor covered by the rubber skin, we performed a series of elastic deformation simulations using FEM. Examples of the geometry and mesh models are shown in Figs. 3 and 4, respectively. In addition, we produced other models to apply to different loading conditions. To reduce analysis cost, we adopted a two-dimensional stress condition for this analysis. Since, in computation, sliding contact between a probe and a skin is not successful, the probe end is connected on the top of the skin.

We assume that Young's moduli of probe, skin, and feeler are 70 GPa, 0.6 MPa, and 3.1 MPa, respectively. The rubber skin's hardness is around 1/5 of the sensing element. Poisson's ratios are 0.35, 0.49, and 0.45, respectively. These properties are adopted to emulate a real tactile sensor that will be described later. In the actual tactile sensor, the rubber skin bottom makes contact with the aluminum dome, but is not glued onto it. The relationship between the columnar feeler and the rubber skin is the same as the relationship between the rubber skin and the aluminum dome. Thus, we assume there is sliding contact for both the relationship between the rubber skin and the aluminum dome and the relationship between the rubber skin and the columnar feeler. Since the conical feeler tip is stuck onto the acrylic dome, the tips are connected to it. The analysis is performed using a function supplemented in CATIA V5.

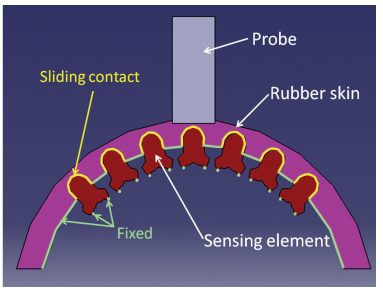

Fig. 3. Example of geometric structure of tactile sensor

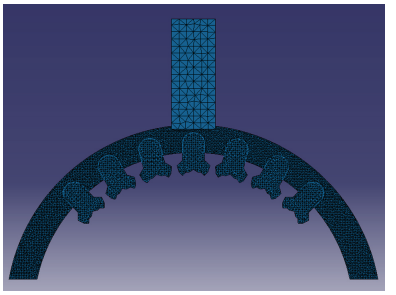

Fig. 4. Mesh model

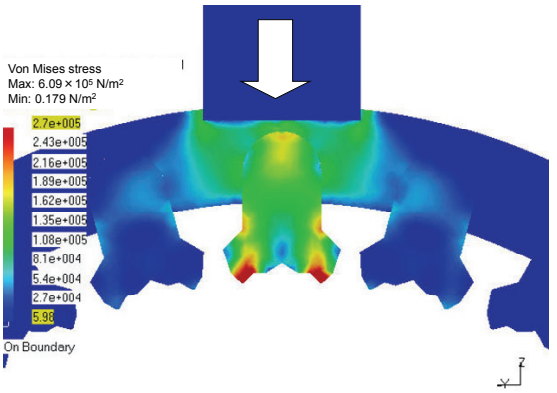

Fig. 5. Normal force applied to parietal sensing element

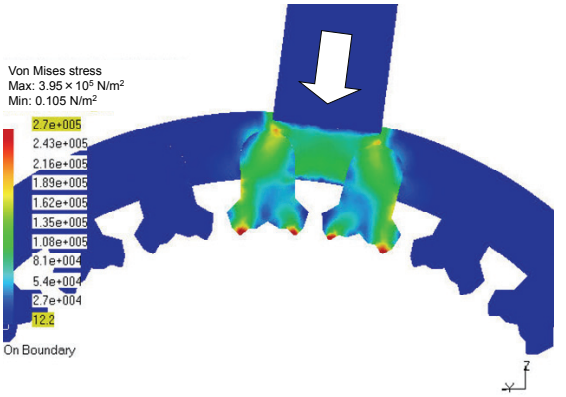

Fig. 6. Normal force applied between two sensing elements

3.2. Numerical Results and Discussion

First, we examined the simplest case in which the probe is set on a sensing element and normal force is applied. Figure 5 shows the numerical results for this case. In Fig. 5, the contour shows the von Mises stress distribution (the unit is N/mm^2). Although the conical tips of the parietal sensing element have high stress, their neighboring feelers do not significantly deform. The maximum to minimum stress ratio of the conical tips is around 6:1. From this result, if the rubber skin is soft enough, interference of the active sensing element will not be obvious for the neighboring sensing elements.

Next, we examined the case in which normal force is applied between two sensing elements (Fig. 6). As shown in Fig. 6, the conical tips of two columnar feelers undergo almost the same stress. If we observe each columnar feeler's conical feeler, the right and left conical feelers undergo almost the same stress. This means that these columnar feelers accept normal force. Thus, this sensor can accept normal force applied between two columnar feelers.

We then examined the case in which a tangential component of force is applied to the skin upon the parietal columnar feeler (Fig. 7). In this simulation, not only normal, but also tangential components of force were applied.

The direction of the tangential component is negative (right to left). If we examine the conical tips beneath the parietal columnar feeler, the left conical tip accepts more stress compared to the right. To examine it precisely, the displacement distribution of the nodal points is shown in Fig. 8. While the deformation stream flows in a perpendicular direction in the left conical tip beneath the parietal columnar feeler, it flows in a horizontal direction in the right conical feeler. This means that the tangential component of force is measured by the difference in the two conical tips' contact.

Furthermore, if we examine the other sensing elements, not including the parietal sensing element, the other conical tips (except for the conical tips beneath the left columnar feeler) receive almost no stress. Although the conical tips beneath the left columnar feeler receive a relatively high amount of stress, the magnitude is around one third of that of the conical tips beneath the parietal columnar feeler. Thus, the tangential component of applied force does not progress to the sensing elements further than the neighboring sensing element.

On the basis of these calculated results, we conclude that the new tactile sensor can accept tactile stimulus between two conical feelers and that the tangential force can be measured even with the rubber skin attached. The ordinal theory[15] assumes that, since skin blurs the stress distribution, tactile sensors should be designed to take into account this blurring and protect the sensor elements. As shown in Figs. 5, 6, and 7, the red color on the contour of the columnar feeler tips indicates stress concentration. As aforementioned, since the columnar feeler hardness is five times greater than the skin and the tip is sharp, strain energy accumulation is not obvious compared to the tip.

This theory was deduced by analysis of homogenous sheet skin and does not consider a complex skin structure for this sensor. Since a different theory for a complex structure will be deduced by FEM analysis, we performed an experimental series that assumes various degrees of skin hardness.

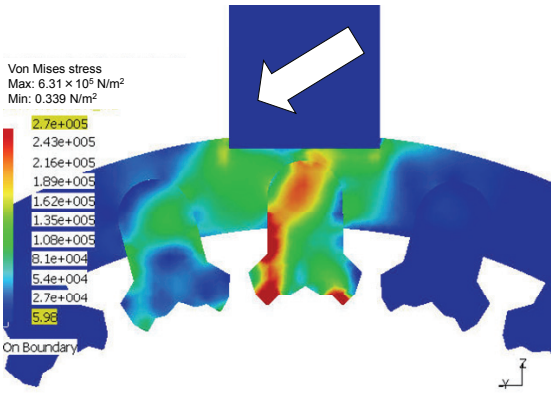

Fig. 7. Tangential force applied to rubber skin over element

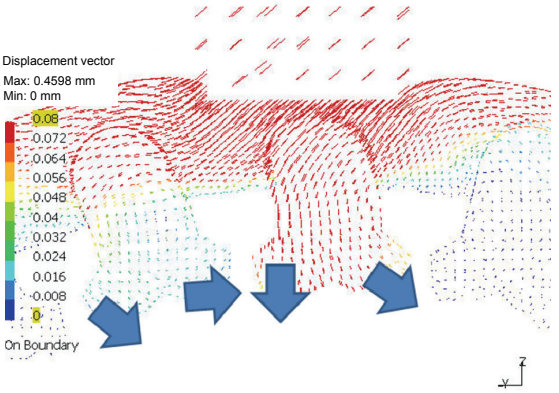

Fig. 8. Distribution of nodal point's displacement

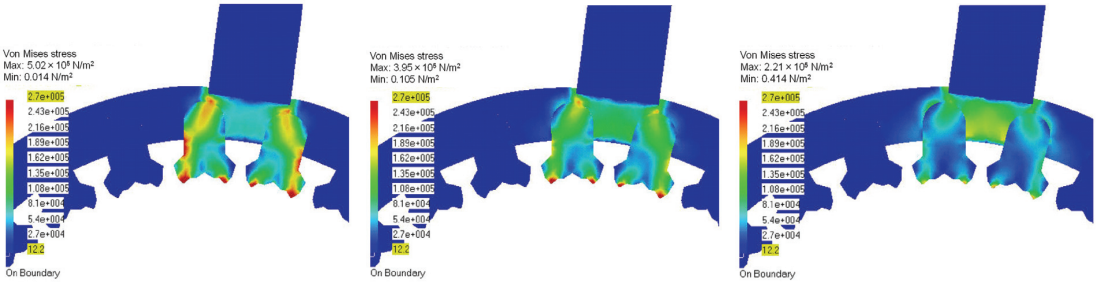

(a) 0.15 MPa (soft) (b) 0.6 MPa (medium) (c) 2.4 MPa (hard)

Fig. 9. Comparison of various skin hardness cases

Three skin hardness cases are compared in Fig. 9. For soft skin, two feelers sustain the most strain energy as opposed to the hard skin case, where the skin sustains the most strain energy. The medium skin has the most appropriate strain energy concentration.

Although we cannot escape the blur of stress distribution when skin is used, the degree of blur is reduced by the design of the skin structure, even for thick skin. Our skin is composed of three layers of varying hardness and has a complex structure of fingerprint ridges on the surface and papillae under the epidermis. Although we did not intend to produce a human mimic sensor when we started this project, our columnar feelers unexpectedly act as papilla.

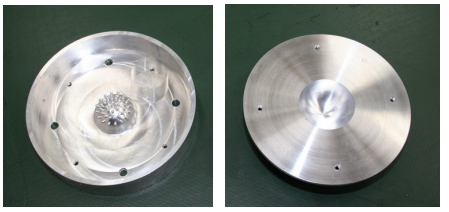

(a) Upper mold (b) Bottom mold

Fig. 10. Molds for skin

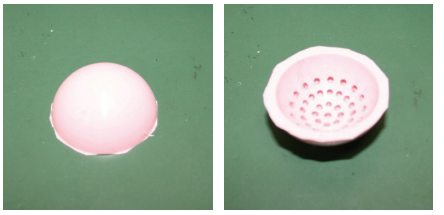

(a) Top view (b) Backside view

Fig. 11. Skin removed from mold after hardening

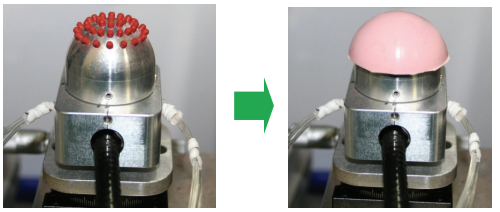

Fig. 12. Optical three-axis tactile sensor covered by rubber skin

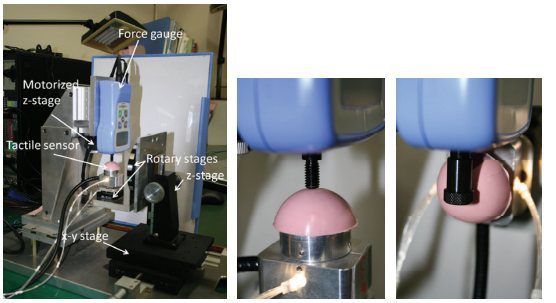

(a) Whole view (b) Normal force test (c) Tangential force test

Fig. 13. Experimental apparatus for loading to sensor

4. Experiments

4.1. Experimental Apparatus and Experimental Procedure

Although the numerical results demonstrate the effectiveness of the rubber skin, experimentation is required to evaluate the new tactile sensor in use because the numerical simulations are based on several assumptions.

First, we created a set of molds to fabricate the rubber skin. Figure 10 shows the upper and bottom mold. After combining unhardened silicon rubber and a catalyst, the mixture is poured between two molds to obtain the hardened silicon of the rubber skin shape shown in Fig. 11. The rubber skin is then attached to the top of the conventional optical three-axis tactile sensor, as shown in Fig. 12.

Next, we assembled an experimental set-up to apply normal and tangential force components to the tactile sensor (Fig. 13(a)). Since the tactile sensor is installed on the rotary stage, normal force can be applied to arbitrary portions of the rubber skin. Figure 13 (b) and (c) show normal and tangential force tests, respectively.

Since the tactile sensor is axis-symmetric shaped, we performed a loading test for several points in a sector, as shown in Fig. 14. We describe typical cases in this paper because there was too much obtained data.

4.2. Experimental Results and Discussion

Figure 15 shows the characteristics of the parietal sensing element when normal force is applied to the parietal portion of the rubber skin. Since feelers other than the parietal columnar feeler are almost zero, there is no crosstalk between the parietal columnar feeler and the other sensing elements.

On the other hand, if force is applied between two sensing elements, some sensing elements generate output, as shown in Fig. 16. While elements #00, #01, #02, and #08 generate output, other feelers do not, as shown in Fig. 16. From this distribution, we conclude that force is applied to the center of elements #00, #01, #02, and #08.

Next, to examine tangential force, *y*-directional tangential force is applied to the parietal potion of the rubber skin in a negative direction after applying 3-N normal force (Fig. 17). In this experiment, -1.6-N *y*-directional tangential force is applied using a motorized *z*-stage. The movement speed of the *z*-stage is 0.1 mm/s. This experiment is continuously performed.

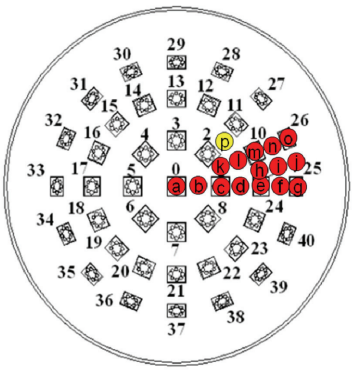

Fig. 14. Examined points on rubber skin; numerals and alphabets show element numbers and loading positions, respectively

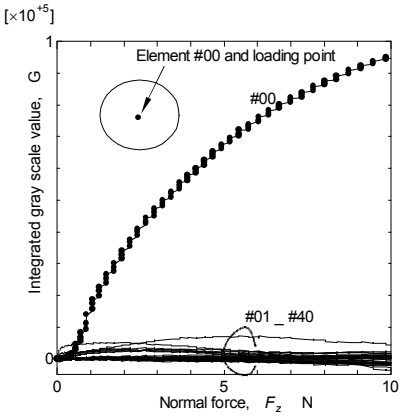

Fig. 15. Relationship between integrated gray scale value and normal force component on element #00 (parietal sensing element)

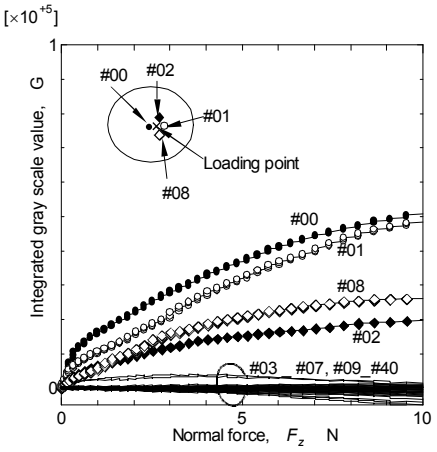

Fig. 16. Relationship between integrated gray scale value and normal force component when force is applied to Point b

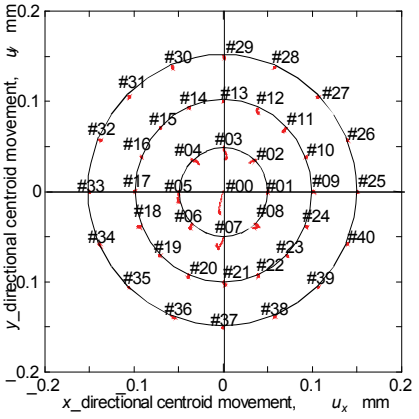

Fig. 17. Trajectory of centroid of each sensing element under increasing tangential force after applying 3-N normal force to parietal rubber skin

As shown in Fig. 17, centroid movements in the center and near the center (elements #00 - #08) are in the downward direction. If the relationship between the tangential force and applied force is assumed to be linear (the graph is abbreviated for lack of space), tangential sensitivity is 0.80 N/mm. This sensitivity value is almost the same as the bare tactile sensor. These experimental results ensure that if the rubber skin is attached onto the tactile sensor, tactile stimulus between two conical feelers and tangential force can be measured.

5. Conclusion

We attached rubber skin onto the sensor surface to protect the sensing element from a high degree of applied force. Although we predicted, prior to this trial, that the skin would reduce sensitivity, FEM analyses demonstrated that sensitivity was not considerably reduced even with thick skin and that the skin induced subsidiary effects, such as insensible-area vanishing and enhancement of columnar feeler stability. This result of insignificant sensitivity reduction seems to be caused by a suitable combination of hard columnar feeler and soft skin.

Based on these simulated results, we produced the columnar-conical feeler-type three-axis tactile sensor equipped with rubber skin. The experimental results showed that the sensor possesses three-axis sensing capability and that the insensible area has vanished. Since the present tactile sensor possesses robustness for power grasp, we will apply it to various tasks, such as daily housework and hospital nursing.

Acknowledgements

The authors gratefully acknowledge the Ministry of Education Malaysia (MOE) for partially funding the research project through the Niche Research Grant Scheme (NRGS) [Ref. No 600-RMI/NRGS 5/3 (1/2013)].

References

1. Ohka, M., Robotic Tactile Sensors. *Wiley Encyclopedia of Computer Science and Engineering*. Editor: Benjamin W. Wah. 2009: **4**: 2454-2461.
2. Hackwood, S., Beni, G., Hornak, L. A., Wolfe, R., and Nelson, T. J. A Torque-sensitive Tactile Array for Robotics. *Int. J. Robotics Research*. 1983: **2**-2: 46-50.
3. Novak, J. L. Initial Design and Analysis of a Capacitive Sensor for Shear and Normal Force Measurement. *1989 IEEE International Conference on Robotics and Automation*. 1989: 137-145.
4. Hakozaki, M. and Shinoda, H. Digital Tactile Sensing Elements Communicating Through Conductive Skin Layers. *2002 International Conference on Robotics and Automation*. 2002: 3813-3817.
5. Yamada, Y. and Cutkosky, M. R. Tactile Sensor with 3-axis Force and Vibration Sensing Function and Its Application to Detect Rotational Slip. *1994 IEEE International Conference on Robotics and Automation*. 1994: 3550-3557.
6. Borovac, B., Nagy, L., and Sabli, M. Contact Tasks Realization by Sensing Contact Forces. *11th CISM-IFToNN Symposium.* 1996: 381-388.
7. Tanaka, Y., Nakai, A., Iwase, E., Goto, T., Matsumoto, K., and Shimoyama, I. Triaxial Tactile Sensor Chips with Piezoresistive Cantilevers Mountable on Curved Surface. *Proceedings of the 4th Asia Pacific Conference on Transducers and Micro/Nano Technologies.* 2008: 1B1-1.
8. Dahiya, R. S., Metta, G., Valle, M., Adami, A., and Lorenzelli, L. Piezoelectric Oxide Semiconductor Field Effect Transistor Touch Sensing Devices. *Applied Physics Letters*. 2009: **95**-3: 034105-034105-3.
9. Hamidullah, M., Cheng, M., Lim, L. S., He, C., Feng, H., and Park, W. MEMS Tri-axial Tactile Sensor Packaging Using Polymer Flexible Cable for Sensorised Guide Wire Application. *2011 IEEE 13th Electronics Packaging Technology Conference (EPTC)*. 2011: 207-210.
10. Kamiyama, K., Vlack, K., Mizota, T., Kajimoto, H., Kawakami, N., and Tachi, S. Vision-based Sensor for Real-time Measuring of Surface Traction Fields. *IEEE Computer Graphics and Applications*. 2005: 68-75.
11. Ohka, M., Kobayashi, H., Takata, J., and Mitsuya, Y. An Experimental Optical Three-axis Tactile Sensor Featured with Hemispherical Surface. *Journal of Advanced Mechanical Design, Systems, and Manufacturing.* 2008: **2**(5): 860-873.
12. Ohka, M., Takata, J., Kobayashi, H., Suzuki, H., Morisawa, N., and Yussof, H. B. Object Exploration and Manipulation Using a Robotic Finger Equipped with an Optical Three-axis Tactile Sensor. *Robotica.* 2009: **27**-5: 763-770.
13. Ohka, M., Mitsuya, Y., Higashioka, I., and Kabeshita, H. An Experimental Optical Three-axis Tactile Sensor for Micro-Robots. *Robotica.* 2005: **23**-4: 457-465.
14. Ohka, M., Matsunaga, T., Nojima, Y., Noda, D., and Hattori, T. Basic Experiments of Three-axis Tactile Sensor Using Optical Flow. *2012 IEEE International Conference on Robotics and Automation*. 2012: 1404-1409.
15. Shimojo, M. Mechanical Filtering Effect of Elastic Cover for Tactile Sensor. *IEEE Trans. on Robotics and Automation.* 1997: **13**-1: 128-132.
16. Tanie, K., Komoriya, K., Kaneko, K., Tachi, S., and Fujikawa, A. A High Resolution Tactile Sensor. *Proc. of 4th Int. Conf. on Robot Vision and Sensor Control*. 1984: 251-256.
17. Ohka, M., Mitsuya, Y., Matsunaga, Y., and Takeuchi, S. Sensing Characteristics of an Optical Three-axis Tactile Sensor under Combined Loading. *Robotica*. 2004: **22**-2: 213-221.